RSC Advances

PAPER

A theoretical search for stable bent and linear structures of low-lying electronic states of the titanium dioxide (TiO₂) molecule†

Chih-Kai Lin,[*ab] **Jun Li,**[c] **Zheyan Tu,**[d] **Xiangyuan Li,**[c] **Michitoshi Hayashi**[e] **and Sheng Hsien Lin**[ab]

In this work geometric optimization and potential energy surface (PES) scan for the TiO₂ molecule were carried out to find out possible stable structures by using quantum chemical calculations. The ground state (S_0 $1\,^1A_1$) has the only equilibrium with a symmetric bent structure, whereas the linear conformer is unstable. The first singlet excited state (S_1 $1\,^1B_2$), on the other hand, possesses two potential minima where one is bent around the Franck–Condon region and the other is linear. The second singlet excited state (S_2 $1\,^1A_2$) has only one minimum which is linear, and at which geometry the first two excited states degenerate. Other low-lying singlet and triplet excited states have been investigated accordingly. Among the functionals applied in the present DFT calculations, B3LYP gave results most close to available experimental data, while some recently developed ones including HSE06, ωB97X-D and CAM-B3LYP were not satisfactory for this small system. *Ab initio* methods such as CASSCF, CASPT2 as well as CCSD-related calculations have been applied, and the latter two showed good results similar to DFT/B3LYP.

Introduction

Titanium dioxide, TiO₂, has attracted wide interest because of its extensive applications as a photocatalyst, its abundance as an interstellar material and its representative character as a transition-metal dioxide compound. Most research focuses on the bulk phase of TiO₂ for its practical application in photochemical reactions and in semiconductor manufacturing. Studies on TiO₂ monomers are relatively few, but recently some high-resolution spectra as well as quantum chemical calculations have been presented, raising more concerns about this prototype molecule.

It has been suggested that the TiO₂ molecule has a bent structure in the ground state according to the measured permanent dipole moment in a very early study.[1] The infrared spectrum of the molecule was then recorded in a neon matrix, indicating two vibrational motions, the symmetric stretching mode (v_1, of the a_1 irreducible representation in the C_{2v} point group) at 962.0 cm⁻¹ and the asymmetric stretching mode (v_3, b_2) at 934.8 cm⁻¹.[2] Later the two modes were revised to 946.9 and 917.1 cm⁻¹, respectively.[3] However, the low-frequency bending mode (v_2, a_1) in the 300 cm⁻¹ range was not observed until very recently.[4] The Ti–O bond length (r_{TiO}) and the O–Ti–O bending angle (θ_{OTiO}) have been determined as 1.651 Å and 111.6°, respectively, in the argon matrix.[5] Theoretical investigations by using density functional theory (DFT), complete active space self-consistent field (CASSCF) and coupled cluster (CC) calculations have all shown consistent results with the experimental ones for the ground state.[6–11]

The situation becomes much more complicated for the excited states. Garkusha *et al.* recorded the electronic absorption spectrum of TiO₂ in a 6 K neon matrix by using halogen and xenon arc lamps, presenting the band origin at 19 084 cm⁻¹ (524 nm, 2.37 eV) for the S_1 $1\,^1B_2 \leftarrow S_0$ $1\,^1A_1$ transition and the progressions of all three modes of the excited state. In addition, they noticed another progression beginning at 15 924 cm⁻¹ (628 nm, 1.97 eV) which was assigned to the linear isomer in its $1\,^1\Sigma_g^+$ ground state.[12] Steimle and Maier's group performed resonance-enhanced multi-photon ionization (REMPI) and laser induced fluorescence (LIF) spectra of the gas-phase molecule, showing that the band origin slightly shifted to 18 655 cm⁻¹ (536 nm, 2.31 eV) but the vibronic progressions were too complicated to recognize at first glance.[4] The newest report by the same group has re-located the 0–0 transition to 17 591 cm⁻¹ (568 nm, 2.18 eV) and assigned several tens of vibronic peaks.[13] There are as yet many minor peaks remaining unassigned, implying that some other low-lying states or conformers might also contribute to the absorption spectrum through possible vibronic and/or spin–orbit couplings.

Theoretical characterizations on the excited states of TiO₂ are quite rare. There are only two computational reports concerning the first singlet excited state (S_1 $1\,^1B_2$) till now. Ramana and

ᵃInstitute of Atomic and Molecular Sciences, Academia Sinica, Taipei, Taiwan, 10617, ROC. E-mail: ethene@gate.sinica.edu.tw
ᵇDepartment of Applied Chemistry, National Chiao Tung University, Hsinchu, Taiwan, 30010, ROC
ᶜCollege of Chemical Engineering, Sichuan University, Chengdu, 61005, P. R. China. E-mail: xyli@scu.edu.cn
ᵈCollege of Chemistry, Sichuan University, Chengdu, 61005, P. R. China. E-mail: tuzheyan@gmail.com
ᵉCenter for Condensed Matter Sciences, National Taiwan University, Taipei, Taiwan, 10617, ROC
† Electronic Supplementary Information (ESI) available. See DOI: 10.1039/c1ra00478f/

Phillips studied the state at the configuration interaction (CI) level, predicting that it lies just 1.63 eV above the ground state, which is much lower than the experimental value, and the equilibrium structure is linear with the bond length 1.73 Å.[14] Grein performed DFT optimization and obtained a bent equilibrium structure with the bond length and bending angle as 1.703 Å and 96.3°, respectively.[9] The adiabatic transition energy to this state was calculated as 2.14 eV, which is close to the most recent experimental report.[13]

For the second singlet excited state (S_2 1 $^1A_2$), two DFT results with different functionals indicated that the bent structure is stable. The bond lengths were calculated both as 1.72 Å and the bending angles as 143.9° and 153.7°, respectively.[9,10] The adiabatic excitation energies for this state were reported as 2.50 eV and 1.85 eV, respectively, where the latter was apparently underestimated. On the other hand, a brief potential energy scan depending on the bending angle showed a very wide and shallow potential basin for this state,[9] implying that the structure shall no longer be a harmonic oscillator and might even be unstable.

In this work, we aimed to identify the possible stable structures of the ground and low-lying excited states. The geometric and electronic properties of TiO_2 monomer would be unveiled with the full optimization and a thorough scan on the potential energy surfaces at the DFT, CAS and CC levels, providing us more insights into the complicated spectroscopic problems.

Computational methods

Three categories of TiO_2 isomers have been reported, that is, the symmetric bent/linear form (oxo, O–Ti–O), the cyclic side-on form (peroxo) and the end-on form (superoxo, Ti–O–O), by calculation (Fig. 1).[15] We mainly focused on the first category since its ground state is at least 4 eV more stable than the other two.[15]

For the optimization and vibrational frequency calculation of the ground state, S_0 1 $^1A_1$, CASSCF, CASPT2 and CCSD(T) have been carried out. The augmented correlation-consistent polarized valence triple-zeta (aug-cc-pVTZ) basis set was
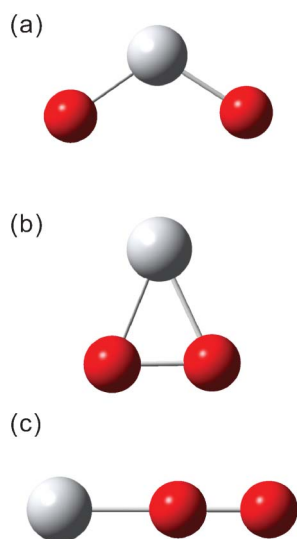
Fig. 1 Three categories of TiO_2 mono-molecular isomers: (a) symmetric bent form, (b) cyclic form and (c) end-on form.

generally applied. The Los Alamos effective core potentials (ECPs) plus MBS or DZ (that is, LanL2MB or LanL2DZ)[16] of the Ti atom were also adopted in some tests. For clarity only aug-cc-pVTZ results are presented here, while the comparison between different basis sets is listed in the ESI.† In CASSCF calculations, the choice of the largest active space included all 16 valence electrons and 14 orbitals, forming the (16,14) active space. A smaller one excluded the inner orbitals mainly composed of the O_{2s} atomic orbitals, giving the (12,12) active space. The global minimum on the potential energy surface was searched according to previously reported geometric data, and other possible local minima were considered as well.

In addition to *ab initio* methods mentioned above, DFT with several different functionals were applied. Besides the commonly accepted B3LYP functional, some recently developed functionals that attracted much interest have also been tested including HSE06,[17,18] which takes screened short-range Coulomb potential and has been applied in TiO_2 crystal systems, and CAM-B3LYP[19] and ωB97X-D,[20] which add in long-range corrections. The results of these new functionals were compared to verify if they could give proper or even better descriptions.

For the first and second singlet excited states, S_1 1 $^1B_2$ and S_2 1 $^1A_2$, time-dependent DFT (TD-DFT), CASSCF, CASPT2 and equation-of-motion CCSD (EOM-CCSD) were applied to localize the minimum and to calculate vibrational modes. The search for equilibrium structures was first around the Franck–Condon (vertical excitation) region and then expanded to other conformers.

In order to understand the characters of the low-lying excited states, a systematic scan on the potential energy surfaces was carried out by changing the geometry of the molecule. Keeping the point group symmetry as C_{2v}, the Ti–O bond length and the O–Ti–O bending angle were varied from 1.50 Å to 2.00 Å and from 80° to 180°, respectively. TD-DFT was applied to locate singlet states up to S_5. CASSCF followed by CASPT2 was done in an eight-state-averaged manner, with two states of each irreducible representation ($^1A_1$, $^1B_1$, $^1B_2$ and $^1A_2$) included.

In the last part of this work, triplet excited states such as T_1 1 $^3B_2$ and T_2 1 $^3A_2$ were also studied. Spin–orbit couplings were calculated to verify possible interactions between neighbor singlet and triplet states. Additionally, cyclic and end-on isomers were looked at briefly. All the quantum chemical calculations were performed with *GAUSSIAN 09*,[21] *MOLPRO 2006*[22] and *ACESII*[23] computational packages.

Results and discussion

Equilibrium geometry and vibrational frequencies of the ground state (S_0 1 $^1A_1$)

The most stable TiO_2 mono-molecular isomer possesses a symmetric bent form within the C_{2v} point group.[15] The O–Ti–O bending angle was measured as 110 $\pm$ 15° in a very early experiment[2] and revised to 113 $\pm$ 5° according to infrared spectra in a following report.[3] In a recent molecular beam microwave spectroscopy experiment by Brünken *et al.*, the rotational spectrum was resolved, and the bending angle and the Ti–O bond length were precisely determined as 111.6° and 1.651 Å, respectively.[5]

Table 1 Calculated equilibrium geometry and vibrational frequencies of the ground state (S_0 1 $^1A_1$) of TiO_2

Level of theory	Equilibrium geometry		Vibrational frequencies			Dipole moment
	r_{TiO}/Å	θ_{OTiO}/°	v_1 (a_1)/cm^{-1}	v_2 (a_1)/cm^{-1}	v_3 (b_2)/cm^{-1}	μ/debye
HF	1.615	118.2	1133.9	335.1	1046.6	7.48
MP2	1.685	107.4	885.9	318.9	922.2	8.59
CASSCF(12,12)	1.654	112.6	1005.8	329.6	945.1	6.92
CASSCF(16,14)	1.648	113.2	1021.8	326.5	940.0	6.98
CASPT2(12,12)	1.672	111.3	924.4	328.0	926.5	6.97
CCSD(T)	1.652	111.2	988.5	333.7	955.2	6.79
B3LYP	1.642	111.7	1023.0	341.9	975.2	6.73
HSE06	1.630	111.7	1046.3	347.9	992.8	6.77
ωB97X-D	1.629	112.5	1055.1	349.7	1000.4	6.86
CAM-B3LYP	1.629	112.2	1059.5	344.9	1004.7	6.84
Expt.		110 ± 15[a]	962.0[a]		934.8[a]	
		113 ± 5[b]	946.9[b]		917.1[b]	
	1.651[c]	111.6[c]		330 ± 6[d]		6.33[d]

[a] Ref. 2. [b] Ref. 3. [c] Ref. 5. [d] Ref. 4.

In this work the optimization and vibrational frequency calculation of the S_0 1 $^1A_1$ ground state were performed at levels including Hartree–Fock (HF), Møller–Plesset second-order perturbation (MP2), CASSCF, CASPT2, CCSD(T) and DFT with several different functionals. Referring to Table 1, the geometric data obtained by HF and MP2 significantly differed from the experimental reference as reported previously,[6] while the other methods performed rather well with deviations within 0.01 Å (0.6%) for the bond length, 2° (2%) for the bending angle and 0.6 debye (9%) for the permanent dipole moment. The choice of basis set and the size of active space showed minor effects in these calculations (Table S1 in the ESI).

The three vibrational modes, *i.e.* symmetric stretching (v_1), bending (v_2) and asymmetric stretching (v_3), have been reported from experimental studies. The calculated harmonic frequencies, also shown in Table 1, were slightly higher by a factor within 5%, which is reasonable. In a critical comparison, CCSD(T) presented the best performance on reproducing both geometric and vibrational properties, and CASSCF, CASPT2 as well as DFT (with all tested functionals) showed acceptable agreements in describing the equilibrium structure.

Furthermore, it was suggested that a symmetric linear structure would exist with the 1 $^1\Sigma_g^+$ ground state in the $D_{\infty h}$ point group.[12] The search for such a stable structure was carried out by fixing the bending angle at 180°, and the converged results were obtained with energies about 2 eV higher than the bent equilibrium. However, as shown in Table 2 (and Table S2), they

all corresponded to a saddle point instead of a true minimum, giving imaginary frequencies to the bending mode. It indicated that there is no stable linear conformer in the ground state, which was implied in a previous energy scan.[9] This point shall be demonstrated more clearly with a thorough potential energy surface scan in the next sections. It is noticed that while the gas-phase linear molecule is unstable, the possibility of stabilization of such a molecule in the inert gas matrix could not be entirely excluded.[12,13]

Vertical excitation energies

The vertical excitation energies of low-lying excited states have been calculated with the ground state equilibrium geometry at several levels of theory including TD-DFT (with different functionals), CASSCF, CASPT2 and EOM-CCSD. The resulted excitation energies and major excitation configurations are listed in Table 3 with a comparison to the previous MRCI report.[9] The oscillator strengths are additionally listed in Table S3 in the ESI. The energetic data and state sequences are rather consistent with each other between TD-B3LYP, CASPT2, EOM-CCSD and MRCI. CASSCF presented a large deviation from the above-mentioned levels of theory in certain excitations, which would be attributed to the lack of dynamical electron correlation. On the other hand, the HSE06 and CAM-B3LYP functionals showed a systematic overestimate of 0.2 to 0.3 eV, while ωB97X-D gave an overestimate of 0.5 to 0.6 eV, for each state compared to B3LYP. It implies that these recently developed functionals which

Table 2 Calculated properties of the linear structure of the ground state (1 $^1\Sigma_g^+$) of TiO_2

Level of theory	Adiabatic energy[a] ΔE_{ad}/eV	Equilibrium geometry		Vibrational frequencies		
		r_{TiO}/Å	θ_{OTiO}/°	v_1 (σ_g^+)/cm^{-1}	v_2 (π_u)/cm^{-1}	v_3 (σ_g^-)/cm^{-1}
MP2	1.852	1.750	180.0	760.5	(340i)	783.5
CASSCF(12,12)	1.507	1.722	180.0	881.6	(340i)	719.4
CASSCF(16,14)	1.419	1.713	180.0	—	—	—
CASPT2(12,12)	1.705	1.735	180.0	—	—	—
CCSD(T)	1.689	1.716	180.0	866.8	(284i)	889.2
B3LYP	1.834	1.707	180.0	896.7	(380i)	901.5
HSE06	1.871	1.698	180.0	915.2	(382i)	908.5
ωB97X-D	1.874	1.696	180.0	929.0	(392i)	914.1
CAM-B3LYP	1.821	1.695	180.0	932.9	(380i)	910.8

[a] With respect to the ground state equilibrium calculated at the same level of theory; without zero-point energy (the same in the following tables).

Table 3 A comparison of vertical excitation energies of low-lying singlet and triplet excited states of TiO_2 calculated at different levels of theory

State	Excitation[a]	TD-B3LYP	TD-HSE06	TD-ωB97X-D	TD-CAM-B3LYP	EOM-CCSD	CASSCF(16,14)	CASPT2(16,14)	MRCI[a]
$1\ ^1B_2$[b]	$6b_2$–$10a_1$	2.672	2.966	3.352	2.939	2.367	1.981	2.386	2.43
$1\ ^1A_2$	$6b_2$–$4b_1$	3.256	3.517	3.730	3.506	3.019	3.654	3.150	3.09
$2\ ^1B_2$	$6b_2$–$11a_1$	3.337	3.645	3.934	3.658	3.191	4.021	3.365	3.21
$2\ ^1A_1$	$9a_1$–$10,11a_1$	3.520	3.799	4.179	3.755	3.294	3.167	3.480	3.13
$1\ ^1B_1$	$3b_1$–$10,11a_1$	3.811	4.114	4.450	4.110	3.547	3.294	3.601	3.57
$2\ ^1B_1$	$9a_1$–$4b_1$	4.028	4.259	4.417	4.212	3.682	4.658	3.979	3.74
$2\ ^1A_2$	$1a_2$–$10,11a_1$	4.116	4.433	4.755	4.409	3.880	3.862	3.948	4.07
$3\ ^1A_1$	$9a_1$–$11a_1$	4.218	4.476	4.651	4.450	3.993	4.321	4.586	3.83
$3\ ^1B_2$	$5b_2$–$10,11a_1$	4.403	4.720	5.011	4.661	4.255	4.574	4.250	4.19
$1\ ^3B_2$	$6b_2$–$10a_1$	2.556	2.834	3.248	2.808	2.324	2.069	2.495	2.40
$1\ ^3A_2$	$6b_2$–$4b_1$	3.133	3.376	3.608	3.376	2.996	3.598	2.991	3.07
$2\ ^3B_2$	$6b_2$–$11a_1$	3.181	3.428	3.748	3.457	3.114	4.017	3.253	3.20
$1\ ^3A_1$	$9a_1$–$10, 11a_1$	3.226	3.435	3.651	3.322	3.072	3.160	3.425	3.12
$1\ ^3B_1$	$3b_1$–$10, 11a_1$	3.551	3.774	4.042	3.741	3.332	3.214	3.612	3.43
$2\ ^3A_1$	$9a_1$–$11a_1$	3.600	3.789	4.232	3.892	3.657	4.201	3.886	3.85
$2\ ^3B_1$	$9a_1$–$4b_1$	3.706	3.920	4.299	3.923	3.474	4.286	3.616	3.59
$3\ ^3A_1$	$3b_1$–$4b_1$	3.845	4.048	4.412	4.080	3.843	4.479	4.449	4.00
$2\ ^3A_2$	$1a_2$–$10, 11a_1$	3.885	4.148	4.508	4.107	3.696	3.665	3.932	3.81
$3\ ^3B_2$	$5b_2$–$10, 11a_1$	4.130	4.338	4.551	4.258	4.044	4.720	4.122	4.02

[a] Major excitation configurations and MRCI data from ref. 9. [b] Experimental vertical excitation energy to this state is 2.46 eV according to ref. 2.

emphasize some important factors in periodic or long-range systems might not be suitable to describe such a small monomolecular case.

According to more reliable methods like EOM-CCSD and CASPT2, the lowest two singlet excited states are unquestionably $S_1\ 1\ ^1B_2$ and $S_2\ 1\ ^1A_2$, and the triplet ones are $T_1\ 1\ ^3B_2$ and $T_2\ 1\ ^3A_2$. The sequence of following excited states slightly differs by levels of theory. Nevertheless the difference is insignificant since the energy gaps between neighboring states are quite small, *i.e.* within 0.2 eV.

One-dimensional potential energy curves

For a more detailed understanding of the energetics of the ground and low-lying excited states, scanning on the potential energy surfaces with respect to geometric changes was performed. In the preliminary test by TD-DFT with the B3LYP functional, the geometry of the TiO_2 molecule was kept symmetric in the C_{2v} point group. The bending angles were set through 40° to 180° with a step of 10°, while the bond lengths were optimized solely for the ground state at each fixed angle. The calculated one-dimensional angle-dependent potential energy curves of $1\ ^1A_1$, $1\ ^1B_2$, $1\ ^1A_2$, $2\ ^1B_2$, $2\ ^1A_1$ and $1\ ^1B_1$ states, which are the lowest six singlet states at the Franck–Condon point, are shown in Fig. 2(a). Our results were rather similar to those reported by Grein[9] except that (1) the $S_2\ 1\ ^1A_2$ state does not have any minimum with the bent structure, and (2) the equilibrium geometry of the $S_3\ 2\ ^1B_2$ state shifts to a larger bending angle. The potential energy curves of corresponding triplet states are illustrated in Fig. 2(b), where the trend resembles that of singlet states.

First singlet excited state ($S_1\ 1\ ^1B_2$)

The electronic configuration of the first singlet excited state, $S_1\ 1\ ^1B_2$, is dominantly composed of the HOMO (#19, $6b_2$) → LUMO (#20, $10a_1$) excitation. A previous calculation showed that the vertical excitation energy is 2.43 eV while the adiabatic
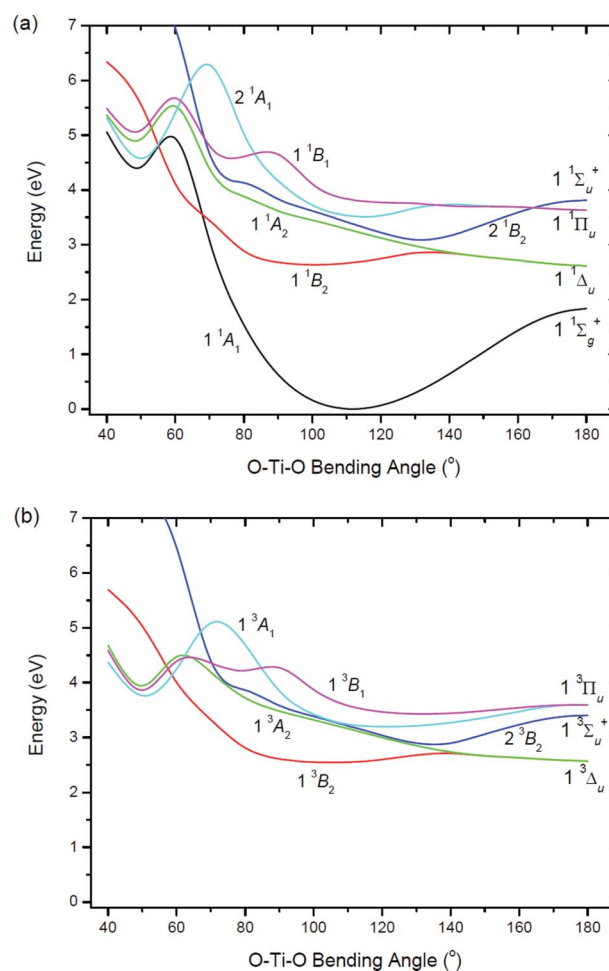
Fig. 2 TD-B3LYP/aug-cc-pVTZ potential energy curves of low-lying (a) singlet and (b) triplet states of TiO_2. The relative energy is with respect to the equilibrium of the $1\ ^1A_1$ ground state.

Table 4 Calculated energies, equilibrium geometry and vibrational frequencies of the first singlet excited state (S_1 1 $^1B_2$) of TiO_2

Level of theory	Vertical energy[a] ΔE_{FC}/eV	Adiabatic energy[a] ΔE_{ad}/eV	Equilibrium geometry r_{TiO}/Å	θ_{OTiO}/°	Vibrational frequencies ν_1 (a_1)/cm^{-1}	ν_2 (a_1)/cm^{-1}	ν_3 (b_2)/cm^{-1}	Dipole moment μ/debye
CASSCF(12,12)	2.223	2.036	1.703	97.7	890.6	228.3	(555i)	3.14
CASSCF(16,14)	2.168	1.918	1.700	95.6	908.9	241.3	(323i)	2.68
CASPT2(12,12)	2.454	2.139	1.727	93.7	—	—	—	3.92
EOM-CCSD	2.370	2.324	1.662	100.4	1009.1	198.3	499.0	4.31
TD-B3LYP	2.672	2.579	1.673	100.2	945.6	212.5	374.7	3.57
TD-HSE06	2.966	2.868	1.662	99.5	966.9	209.6	390.3	3.58
TD-ωB97X-D	3.352	3.278	1.670	111.7	920.7	115.9	339.7	5.19
TD-CAM-B3LYP	2.939	2.874	1.646	110.0	10918.8	(494i)	10494.3	15.24
BPW91[b]	—	2.14	1.703	96.3	875	196	480	5.07
Expt.	2.46[c]	2.37[d]			836[d]	201[d]	498[d]	
		2.31[e]	1.704[e]	100.1[e]				2.55[e]
		2.18[f]			876[f]	184[f]	316[f]	

[a] With respect to the ground state equilibrium calculated at the same level of theory. [b] Ref. 9, with the 6-311++G(3df) basis set. [c] Ref. 2. [d] Ref. 12. [e] Ref. 4. [f] Ref. 13.

energy is 2.14 eV, indicating that the equilibrium geometry of this state locates around the Franck–Condon region with the bond length (1.703 Å) slightly longer and the bending angle (96.3°) smaller than the ground state, and the vibrational modes are somewhat relaxed.[9] These predictions were in good agreement with a recent spectroscopic measurement which determined the adiabatic energy, bond length and bending angle as 2.18 eV, 1.704 Å and 100.1°, respectively.[4,13] In our work, TD-DFT, CASSCF, CASPT2 and EOM-CCSD were applied to investigate the properties of this equilibrium structure, and the results were generally consistent with previous findings as shown in Table 4.

In the case of TD-DFT calculations, B3LYP and HSE06 functionals achieved similar geometry although the latter somewhat overestimated the excitation energy. ωB97X-D gave apparent overestimates in energies, and CAM-B3LYP failed to verify this equilibrium. As for *ab initio* methods, the major problems are that CASSCF always converged with an imaginary-frequency vibrational mode for this state (and for all following excited states investigated in this work), and that CASPT2 could not afford frequency calculation. Despite these failures, the TD-DFT and EOM-CCSD data as well as experimental reports are enough to convince us of the existence and stability of such an equilibrium. Moreover, it is noticed that CASSCF (incidentally) well reproduced the permanent dipole moment which was measured as 2.55 debye[4] while TD-B3LYP, TD-HSE06 and CASPT2 gave overestimates of about 50%, although this had only a minor influence on the energetic and geometric results.

In addition to the bent equilibrium, other possible stable conformers of this state have been searched. A second minimum was found with a symmetric linear structure at all levels of theory. To our surprise, this conformer is nearly isoenergetic with the bent one, showing that the "linearization energy" is almost zero or even negative as listed in Table 5, which is much smaller than previously estimated 0.42 eV.[9] Within the computational error, the linear form might be even more stable than the bent form. This implies that the linear conformer of the first singlet excited state, rather than that of the ground state, could be a candidate that contributes to the minor peaks as well as to the red of band origin on the S_1 1 $^1B_2$ ← S_0 1 $^1A_1$ absorption spectrum.

Second singlet excited state (S_2 1 $^1A_2$)

To the second singlet excited state, S_2 1 $^1A_2$, there has not been any experimental analysis yet. A previous calculation suggested that the equilibrium is located at the bond length of 1.724 Å and the bending angle of 143.9°.[9] However, according to the brief potential scan with optimized bond length at varied bending angle in the same report, the energy of this state just decreased smoothly as the angle increased and formed a very wide, extremely shallow potential basin between ∼130° to 180°. The linearization energy was reported to be only 0.06 eV for this state, probably within the computational error.

In our work, we could not find any stable bent conformer at any TD-DFT level. The optimization process in fact converged

Table 5 Calculated properties of the linear structure of the first singlet excited state (1 $^1\Delta_u$) of TiO_2

Level of theory	Adiabatic energy[a] ΔE_{ad}/eV	Linearization energy[b] ΔE_{lin}/eV	Equilibrium geometry r_{TiO}/Å	θ_{OTiO}/°	Vibrational frequencies ν_1 (σ_g^+)/cm^{-1}	ν_2 (π_u)/cm^{-1}	ν_3 (σ_g^-)/cm^{-1}
CASSCF(12,12)	2.026	−0.010	1.735	180.0	782.9	(59i)	173.4
CASSCF(16,14)	2.039	0.121	1.735	180.0	782.7	(61i)	292.6
CASPT2(12,12)	2.153	0.014	1.749	180.0	—	—	—
EOM-CCSD	2.387	0.063	1.684	180.0	887.9	297.3	879.4
TD-B3LYP	2.609	0.030	1.700	180.0	837.2	253.8	658.8
TD-HSE06	2.865	−0.003	1.688	180.0	853.2	215.8	701.6
TD-ωB97X-D	2.976	−0.302	1.684	180.0	877.3	225.7	789.7
TD-CAM-B3LYP	2.812	−0.062	1.682	180.0	873.2	233.9	820.7
BPW91[c]	2.56	0.42	1.728	180.0	—	—	—

[a] With respect to the ground state equilibrium calculated at the same level of theory. [b] With respect to the local minimum around the Franck–Condon region of the same electronic state surface. [c] Ref. 9, with the 6-311++G(3df) basis set.

Table 6 Calculated energies, equilibrium geometry and vibrational frequencies of the second singlet excited state (S_2 1 $^1A_2$) of TiO_2

Level of theory	Vertical energy[a] ΔE_{FC}/eV	Adiabatic energy[a] ΔE_{ad}/eV	Equilibrium geometry		Vibrational frequencies[b]			Dipole moment μ/debye
			r_{TiO}/Å	θ_{OTiO}/°	v_1 (a_1)/cm^{-1}	v_2 (a_1)/cm^{-1}	v_3 (b_2)/cm^{-1}	
CASSCF(12,12)	4.081	3.629	1.750	103.0	633.3	320.4	(2718i)	4.64
CASSCF(16,14)	4.056	3.527	1.745	102.0	—	—	—	3.73
CASPT2(12,12)	3.872	3.401	1.774	104.2	—	—	—	5.34
EOM-CCSD	2.964	2.387	1.684	180.0^c	887.9	297.3	879.4	0.00
TD-B3LYP	3.256	2.609	1.701	180.0^c	837.1	254.0	658.7	0.00
TD-HSE06	3.517	2.865	1.689	180.0^c	853.0	216.0	701.3	0.00
TD-ωB97X-D	3.730	2.980	1.679	179.8	853.5	237.8	751.8	0.06
TD-CAM-B3LYP	3.506	2.812	1.683	179.9	873.0	234.4	820.5	0.01
BPW91^d	—	2.50	1.724	143.9	767	127	575	—

^{a} With respect to the ground state equilibrium calculated at the same level of theory. ^{b} In the case of linear structure, the three vibrational modes have the symmetry of σ_g^+, π_u and σ_g^-, respectively. ^{c} Degenerate with S_1 1 $^1B_2$, both belonging to the doubly degenerate state 1 $^1\Delta_u$ of the $D_{\infty h}$ point group for the linear structure. ^{d} Ref. 9, with the 6-311++G(3df) basis set.

to the linear form, at which geometry the S_2 1 $^1A_2$ and S_1 1 $^1B_2$ states become degenerate and correlate to the 1 $^1\Delta_u$ state of the $D_{\infty h}$ point group. The only stable form found for the S_2 1 $^1A_2$ state was therefore essentially the same as the linear structure of the S_1 1 $^1B_2$ state. EOM-CCSD gave the same consequence as TD-DFT which are summarized in Table 6. It is noticed that these outcomes are slightly different from Table 5, originating from computational errors under different initial symmetry settings (C_{2v} vs. $D_{\infty h}$). CASSCF and CASPT2, on the other hand, indicated a non-linear equilibrium point with the bond angle of $\sim 103°$. Unfortunately the calculated vibrational frequency of the asymmetric stretching mode was imaginary from CASSCF and unavailable from CASPT2, hence the existence of a stable bent conformer of this electronic state remains questionable.

Two-dimensional potential energy surface scan

The potential energy surfaces of the ground and low-lying singlet excited states, depending not only on bending angles but also on bond lengths, were then extensively considered. Following the simple one-dimensional scan described above, the two-dimensional TD-DFT scan with the B3LYP functional was carried out where the bond lengths varied from 1.50 Å to 2.00 Å with a step of 0.05 Å and the bending angles from 80° to 180° with a step of 5°. The energies of the above-mentioned six singlet states were calculated simultaneously at each geometric point. The shapes of these surfaces are illustrated in Fig. 3.

It is clearly seen that the S_0 1 $^1A_1$ ground state possesses only one minimum which has a symmetric bent structure. The linear conformer is located on a saddle point of the ground state surface: it is a minimum along the symmetric stretching coordinate but a barrier top along the bending coordinate. The S_1 1 $^1B_2$ state, on the other hand, possesses two minima, one being around the Franck–Condon region (r = 1.673 Å, θ = 100.2° and ΔE_{ad} = 2.579 eV) and the other being linear (r = 1.700 Å, θ = 180.0° and ΔE_{ad} = 2.609 eV). As noted above, these two structures are almost isoenergetic. The linearization energy is just 0.03 eV, although there is a barrier about 0.25 eV between the two conformers.

The energy of the S_2 1 $^1A_2$ state slides down smoothly as the bending angle increases up to 180°, at which point the state reaches its only minimum degenerate with the 1 $^1B_2$ state (r = 1.700 Å, θ = 180.0° and ΔE_{ad} = 2.609 eV). The S_3 2 $^1B_2$ state has only one minimum whose bending angle is larger than the

ground equilibrium (r = 1.680 Å, θ = 130.6° and ΔE_{ad} = 3.066 eV). In fact this geometry is located in a potential pit, which is much like the coupling region between the two $^1B_2$ surfaces (S_1 and S_3) with the energy difference of ~ 0.2 eV. The potential shapes of S_4 2 $^1A_1$ and S_5 1 $^1B_1$ states are somewhat similar to those of S_0 1 $^1A_1$ and S_1 1 $^1B_2$ states, respectively, although the potential wells of the higher excited states are much shallower.

It should be noticed that a potential minimum obtained in such a two-dimensional scan does not always guarantee a truly stable structure because there is still a third degree of freedom, i.e. the coordinate of asymmetric stretching motion, which has not been scanned. To check whether the geometry at the minimum is stable, the full optimization has to be executed. In this work we have made sure that the minimum points on the S_0 to S_3 surfaces do correspond to stable structures, and thus the two-dimensional potential scan could provide meaningful insights into the characters of these states.

In addition to TD-DFT, CASSCF potential energy surface scan was carried out in the same geometric range, and in order to count in dynamical electron correlation, CASPT2 was also applied. The active space was constructed of 12 electrons and 12 orbitals in the scan. The state-average calculation included two $^1A_1$, two $^1B_1$, two $^1B_2$ and two $^1A_2$ states, which are the lowest eight states around the ground equilibrium. It was noticed that the CAS procedure depends subtly on the averaged states, and the results may alter a lot if other "unwanted" states, e.g. the 3 $^1A_1$ state which was not counted in, lie below any of the chosen eight states when the geometry is far from the ground equilibrium. This effect caused the surfaces to be rougher than those obtained by TD-DFT, and the data of the highest states were unreliable. Fortunately it had a relatively smaller influence on the ground and lower excited states. The potential energy surfaces of the first six singlet states scanned by multi-reference multi-state CASPT2(12,12) are generally similar to the TD-DFT results, and hence are illustrated as Fig. S1 in the ESI†.

Triplet states and spin–orbit couplings

It has been reported that triplet excited states lie extremely close to the corresponding singlet excited states.[9,14] For example, the vertical excitation energies of S_1 1 $^1B_2$ and T_1 1 $^3B_2$ states were found to be 2.43 and 2.40 eV, respectively, and those of S_2 1 $^1A_2$ and T_2 1 $^3A_2$ states were 3.09 and 3.07 eV, respectively, by the

(a) $1\,^1A_1$

(b) $1\,^1B_2$

(c) $1\,^1A_2$

(d) $2\,^1B_2$

(e) $2\,^1A_1$

(f) $1\,^1B_1$
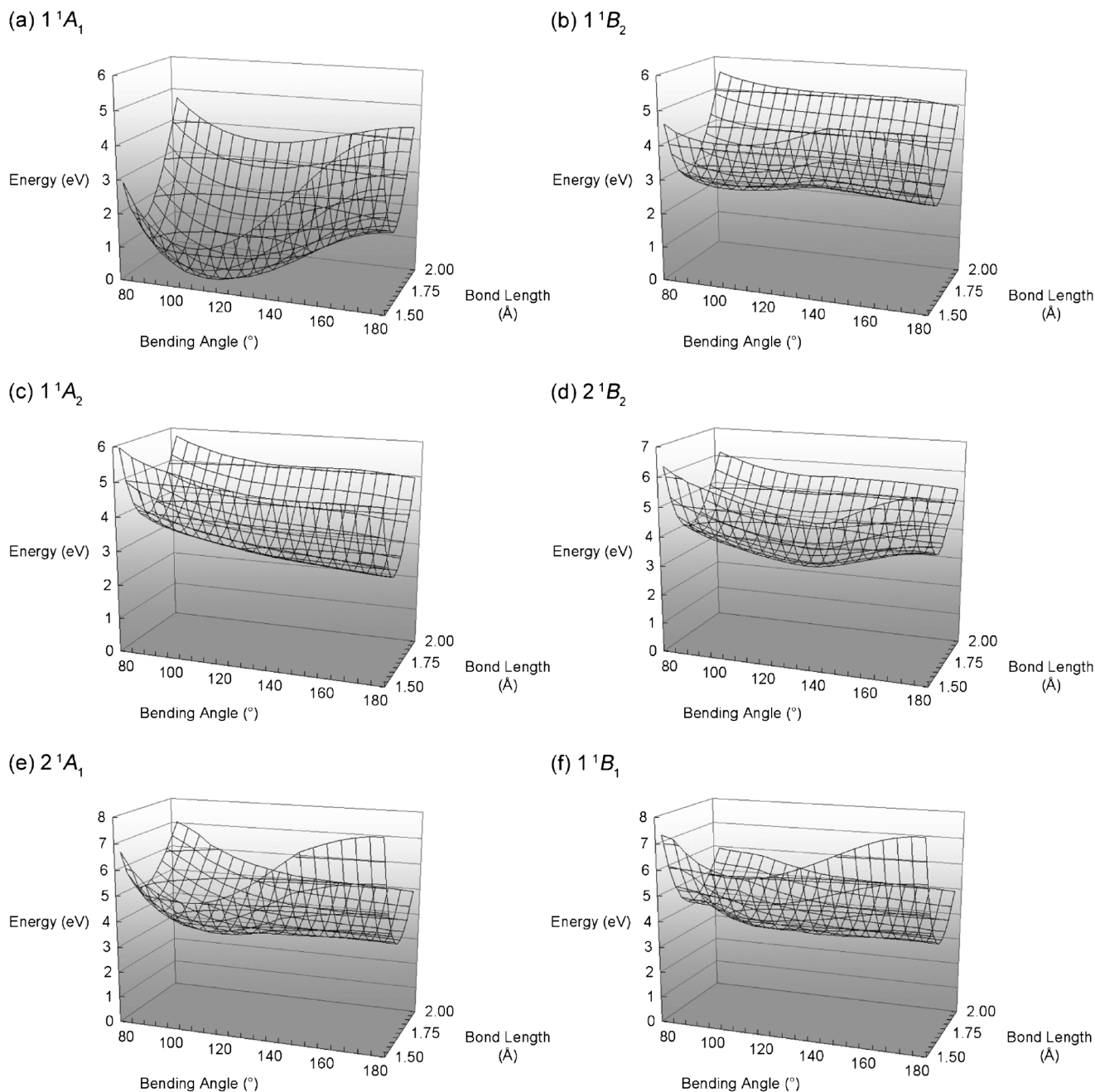
Fig. 3   Two-dimensional TD-B3LYP/aug-cc-pVTZ scan on the potential energy surfaces of the lowest singlet states of TiO_2.

MRCI calculation.[9] In our TD-DFT calculations, the same trend was obtained as introduced in Table 3, where the energy difference between the closest pair of singlet and triplet states, *e.g.* $1\,^1B_2$ and $1\,^3B_2$, is $\sim$0.1 eV. Furthermore, the equilibrium geometries and related features of the lowest two triplet states have been calculated at this level as listed in Table 7. The geometric and energetic properties of these triplet states are seen very similar to the corresponding singlet states (*cf.* Tables 4 and 6) as expected.

Since the neighboring states of the same spatial symmetry but different spin multiplicity are nearly isoenergetic, it is queried if these states could interact with each other through spin–orbit coupling and consequently induce level-splitting and numerous absorption/emission spectral peaks which fit the experimental

observation. This could be verified by the spin–orbit coupling Hamiltonian, $\hat{H}_{SO} = \sum \xi \cdot \hat{\mathbf{L}} \cdot \hat{\mathbf{S}}$, where the summation runs over all electrons, ξ is the potential parameter, and $\hat{\mathbf{L}}$ and $\hat{\mathbf{S}}$ are the orbital and spin angular momentum operators, respectively. It is found that the x, y and z components of $\hat{\mathbf{L}} \cdot \hat{\mathbf{S}}$ transform as B_2, B_1 and A_2, respectively, in the C_{2v} point group. As a result, the spin–orbit coupling between states of the same spatial term but different spins is zero, *e.g.* $\langle \Phi^0_{1B_2} | \hat{H}_{SO} | \Phi^0_{3B_2} \rangle = 0$ where Φ^0 denotes the zeroth-order adiabatic electronic wavefunction, since the totally symmetric term in the spatial part of the operator is not available.

How about the spin–orbit coupling between states of different spatial terms? In this work it has been calculated in a perturbative manner at the CASSCF level including five states:

Table 7 Calculated properties of the lowest two triplet states, T_1 1 $^3B_2$ and T_2 1 $^3A_2$, of TiO_2

State	Level of theory	Vertical energy[a] ΔE_{FC}/eV	Adiabatic energy[a] ΔE_{ad}/eV	Equilibrium geometry		Vibrational frequencies[b]			Dipole moment μ/debye
				r_{TiO}/Å	θ_{OTiO}/°	ν_1 (a_1)/cm^{-1}	ν_2 (a_1)/cm^{-1}	ν_3 (b_2)/cm^{-1}	
T_1 1 $^3B_2$	CASSCF(16,14)	2.003	1.781	1.694	95.3	925.7	235.6	(830i)	1.97
	EOM-CCSD	2.324	2.135	1.660	101.9	1003.7	174.2	460.5	4.12
	TD-B3LYP	2.556	2.500	1.671	103.0	937.3	175.9	370.7	3.49
	BPW91[c]	—	2.19	1.700	96.6	882	192	457	—
T_2 1 $^3A_2$	CASSCF(16,14)	3.887	3.402	1.741	102.8	—	—	—	3.55
	EOM-CCSD	2.996	2.402	1.684	180.0	886.7	288.0	862.1	0.00
	TD-B3LYP	3.133	2.609	1.699	180.0	839.8	251.6	663.0	0.00
	BPW91[c]	—	2.53	1.722	143.7	772	131	561	—

[a] With respect to the global minimum (S_0 1 $^1A_1$ equilibrium) calculated at the same level of theory. [b] In the case of linear structure, the three vibrational modes have the symmetry of σ_g^+, π_u and σ_g^-, respectively. [c] Ref. 9, with the 6-311++G(3df) basis set.

the ground, the first two singlet excited and the first two triplet excited states. The spin–orbit coupled results showed negligible shifts in energy eigenvalues of these states, say, less than 0.2 cm^{-1}. Therefore the couplings could be omitted from this system, indicating that the effect contributes extremely little to spectral peaks. A related phenomenon is that the phosphorescence emission, which is preceded by singlet–triplet intersystem crossing through spin–orbit coupling, should be rather weak and hardly observed.

Other categories of isomers

In addition to symmetric bent/linear structures, the cyclic (oxo) and end-on (superoxo) isomers of the TiO_2 molecule were briefly examined. The geometries of the lowest singlet and triplet states were optimized at the DFT level with the B3LYP functional. As shown in Table 8, the geometric and energetic properties obtained in this work are in good agreement with previous theoretical studies.[9,10,15] For the cyclic isomers, the lowest triplet state is slightly more stable than the singlet one. The Ti–O bond length of the former is slightly longer than the latter while the O–Ti–O angles are both around 48°. For the end-on isomers, both of its lowest triplet and singlet states have the linear structure. Among all these isomers, the cyclic one in its 1 $^3A_1$ state has the lowest equilibrium energy, yet is 3.8 eV higher than the global minimum belonging to the symmetric bent isomer. As a result, none of them could be expected to make an important contribution to the pronounced absorption band around 2.3 eV.

Conclusion

In this work the geometric and energetic properties of the ground and low-lying electronic excited states of the titanium dioxide mono-molecule have been investigated at several levels of theory including DFT and TD-DFT with different functionals, CASSCF and CASPT2, CCSD(T) and EOM-CCSD. A two-dimensional potential energy surface scan was carried out to check the energy dependence on both the bond length and the bending angle. The global minimum was found as a symmetric bent O–Ti–O structure belonging to the S_0 1 $^1A_1$ ground state with the equilibrium bond length of 1.65 Å and the bending angle of 111°, in good agreement with previous experimental and theoretical reports. A symmetric linear conformer was also found on the ground state potential surface but attributed to a saddle point rather than a true minimum. For the first singlet excited state, S_1 1 $^1B_2$, two nearly isoenergetic minima were obtained, one being around the Franck–Condon vertical excitation region and the other linear. For the second singlet excited state, S_2 1 $^1A_2$, there is not any stable bent structure. The only stable one is linear, at which point this surface degenerates with the first excited state.

Comparing the performances of different levels of theory, all methods achieved very similar results for the ground state. As for excited states, EOM-CCSD appear to be most reliable in both energetic and geometric data. CASSCF fails in excitation energies attributed to lack of dynamical electron correlation,

Table 8 Calculated properties of cyclic and end-on isomers of TiO_2

Isomer	State	Level of theory	Adiabatic energy[a] ΔE_{ad}/eV	Equilibrium geometry			Vibrational frequencies[c]			Dipole moment μ/debye
				r_{TiO}/Å	r_{OO}/Å	θ/°[b]	ν_1 (a_1)/cm^{-1}	ν_2 (a_1)/cm^{-1}	ν_3 (b_2)/cm^{-1}	
Cyclic	1 $^3A_1$	B3LYP	3.859	1.821	1.453	47.0	953.0	704.0	520.3	4.92
		B1LYP[d]	3.884	1.820	1.454	47.1	—	—	—	—
		BPW91[e]	4.460	1.829	1.459	47.0	915	665	493	4.59
		BPW91[f]	4.160	1.826	1.450	46.8	939	676	504	—
	1 $^1A_1$	B3LYP	4.405	1.785	1.473	48.8	936.0	681.2	629.7	3.84
		B1LYP[d]	4.491	1.785	1.474	48.0	—	—	—	—
		BPW91[f]	4.720	1.789	1.467	48.4	930	663	633	3.70
End-on	1 $^3\Pi$	B3LYP	5.349	1.712	1.305	180.0	584.5	217.1	1145.9	6.34
		B1LYP[d]	5.292	1.719	1.304	180.0	—	—	—	—
		BPW91[e]	5.510	1.721	1.306	180.0	582	210	1219	—
	1 $^1\Sigma_g$	B3LYP	6.435	1.658	1.285	180.0	668.3	276.5	1281.9	5.28
		B1LYP[d]	6.467	1.656	1.288	180.0	—	—	—	—

[a] With respect to the global minimum (S_0 1 $^1A_1$ equilibrium) of the symmetric bent isomer. [b] Bending angle refers to θ_{OTiO} for cyclic isomers and θ_{TiOO} for end-on isomers. [c] In the case of end-on isomers, the three vibrational modes have the symmetry of σ_g, π and σ_g, respectively. [d] Ref. 10, with the 6-311+G(d) basis set. [e] Ref. 15, with the 6-311+G(d) basis set. [f] Ref. 9, with the 6-311+G(3df) basis set.

whereas CASPT2 effectively revises this point. TD-DFT with the B3LYP functional is trustworthy, while HSE06, ωB97X-D and CAM-B3LYP functionals always overestimate excitation energies, implying that introducing correction factors which are important in periodic crystal or long-range systems into this simple molecular monomer might not be suitable.

In order to clarify the cause of spectral peaks to the red of the $S_1\ 1\ ^1B_2 \leftarrow S_0\ 1\ ^1A_1$ absorption system around 2.3 eV, influences from triplet states and other categories of isomers have been further considered. The triplet excited states were found quite close in energy and similar in structure to their corresponding singlet excited states. Spin–orbit couplings between states of the same spatial symmetry are zero and those between any other low-lying states are negligible. Furthermore, cyclic and end-on isomers of titanium dioxide were briefly examined, and all resulted energies are much higher than the equilibria of the S_0 to S_2 states of the symmetric bent/linear isomer. In consequence, these factors could not give satisfactory interpretation of the spectral peaks to the red. The cause of those low-energy absorption transitions then could be attributed only to singlet states with the symmetric geometry. We suggest that the linear conformer of the ground state might be excluded for its instability, while the linear one of the first singlet excited state might contribute according to its possible low energy.

References

1 M. Kaufman, J. Muenter and W. Klemperer, *J. Chem. Phys.*, 1967, **47**, 3365.
2 N. S. McIntyre, K. R. Thompson and W. Weltner, Jr., *J. Phys. Chem.*, 1971, **75**, 3243.
3 G. V. Chertihin and L. Andrews, *J. Phys. Chem.*, 1995, **99**, 6356.
4 H. Wang, T. C. Steimle, C. Apetrei and J. P. Maier, *Phys. Chem. Chem. Phys.*, 2009, **11**, 2649.
5 S. Brünken, H. S. P. Muller, K. M. Menten, M. C. McCarthy and P. Thaddeus, *Astrophys. J.*, 2008, **676**, 1367.
6 R. Bergström, S. Lunell and L. A. Eriksson, *Int. J. Quantum Chem.*, 1996, **59**, 427.
7 M. Rosi, C. W. Bauschlicher, G. V. Chertihin and L. Andrews, *Theor. Chem. Acc.*, 1998, **99**, 106.
8 Z.-W. Qu and G.-J. Kroes, *J. Phys. Chem. B*, 2006, **110**, 8998.
9 F. Grein, *J. Chem. Phys.*, 2007, **126**, 034313.
10 E. L. Uzunova, H. Mikosch and G. St. Nikolov, *J. Chem. Phys.*, 2008, **128**, 094307.
11 Y. Liu, Y. Yuan, Z. Wang, K. Deng, C. Xiao and Q. Li, *J. Chem. Phys.*, 2009, **130**, 174308.
12 I. Garkusha, A. Nagy, Z. Guennoun and J. P. Maier, *Chem. Phys.*, 2008, **353**, 115.
13 X. Zhuang, A. Le, T. C. Steimle, R. Nagarajan, V. Gupta and J. P. Maier, *Phys. Chem. Chem. Phys.*, 2010, **12**, 15018.
14 M. V. Ramana and D. H. Phillips, *J. Chem. Phys.*, 1988, **88**, 2637.
15 G. L. Gutsev, B. K. Rao and P. Jena, *J. Phys. Chem. A*, 2000, **104**, 11961.
16 P. J. Hay and W. R. Wadt, *J. Chem. Phys.*, 1985, **82**, 270.
17 J. Heyd, G. Scuseria and M. Ernzerhof, *J. Chem. Phys.*, 2003, **118**, 8207.
18 J. Heyd, G. E. Scuseria and M. Ernzerhof, *J. Chem. Phys.*, 2006, **124**, 219906.
19 T. Yanai, D. Tew and N. Handy, *Chem. Phys. Lett.*, 2004, **393**, 51.
20 J.-D. Chai and M. Head-Gordon, *Phys. Chem. Chem. Phys.*, 2008, **10**, 6615.
21 M. J. Frisch, G. W. Trucks, H. B. Schlegel, G. E. Scuseria, M. A. Robb, J. R. Cheeseman, G. Scalmani, V. Barone, B. Mennucci, G. A. Petersson, H. Nakatsuji, M. Caricato, X. Li, H. P. Hratchian, A. F. Izmaylov, J. Bloino, G. Zheng, J. L. Sonnenberg, M. Hada, M. Ehara, K. Toyota, R. Fukuda, J. Hasegawa, M. Ishida, T. Nakajima, Y. Honda, O. Kitao, H. Nakai, T. Vreven, J. A. Montgomery, Jr., J. E. Peralta, F. Ogliaro, M. Bearpark, J. J. Heyd, E. Brothers, K. N. Kudin, V. N. Staroverov, R. Kobayashi, J. Normand, K. Raghavachari, A. Rendell, J. C. Burant, S. S. Iyengar, J. Tomasi, M. Cossi, N. Rega, J. M. Millam, M. Klene, J. E. Knox, J. B. Cross, V. Bakken, C. Adamo, J. Jaramillo, R. Gomperts, R. E. Stratmann, O. Yazyev, A. J. Austin, R. Cammi, C. Pomelli, J. W. Ochterski, R. L. Martin, K. Morokuma, V. G. Zakrzewski, G. A. Voth, P. Salvador, J. J. Dannenberg, S. Dapprich, A. D. Daniels, Ö. Farkas, J. B. Foresman, J. V. Ortiz, J. Cioslowski and D. J. Fox, *Gaussian 09 (Revision A.02)*, Gaussian, Inc., Wallingford, CT, 2009..
22 H.-J. Werner, P. J. Knowles, R. Lindh, F. R. Manby, M. Schütz, P. Celani, T. Korona, G. Rauhut, R. D. Amos, A. Bernhardsson, A. Berning, D. L. Cooper, M. J. O. Deegan, A. J. Dobbyn, F. Eckert, C. Hampel, G. Hetzer, A. W. Lloyd, S. J. McNicholas, W. Meyer, M. E. Mura, A. Nicklaβ, P. Palmieri, R. Pitzer, U. Schumann, H. Stoll, A. J. Stone, R. Tarroni and T. Thorsteinsson, *Molpro, a package of ab initio programs designed by H.-J. Werner and P. J. Knowles*, Version 2006.1, 2006.
23 J. F. Stanton, J. Gauss, J. D. Watts, P. G. Szalay, R. J. Bartlett with contributions from A. A. Auer, U. Benedikt, D. B. Bernholdt, O. Christiansen, K. Franzmann, M. E. Harding, M. Heckert, O. Heun, C. Huber, D. Jonsson, J. Jusélius, W. J. Lauderdale, D. Matthews, T. Metzroth, C. Michauk, D. P. O'Neill, D. R. Price, E. Prochnow, K. Ruud, F. Schiffmann, S. Stopkowicz, A. Tajti, M. E. Varner, J. Vázquez, F. Wang and the integral packages MOLECULE (J. Almlöf, P. R. Taylor), PROPS (P. R. Taylor), ABACUS (T. Helgaker, H. J. A. Jensen, P. Jørgensen and J. Olsen) and ECP routines by A. V. Mitin and C. van Wüllen.